Title

Proteomic, mechanical, and biochemical characterization of cartilage development

Authors

Bielajew, Benjamin J
Donahue, Ryan P
Lamkin, Elliott K
et al.

Publication Date

2022-04-01

DOI

10.1016/j.actbio.2022.02.037

Peer reviewed

HHS Public Access

Author manuscript

Acta Biomater. Author manuscript; available in PMC 2022 May 27.

Published in final edited form as:

Acta Biomater. 2022 April 15; 143: 52–62. doi:10.1016/j.actbio.2022.02.037.

Proteomic, Mechanical, and Biochemical Characterization of Cartilage Development

Benjamin J. Bielajew[1,*], **Ryan P. Donahue**[1,*], **Elliott K. Lamkin**[2], **Jerry C. Hu**[1], **Vincent C. Hascall**[2], **Kyriacos A. Athanasiou**[1,†]

[1]Department of Biomedical Engineering, University of California Irvine, Irvine, CA, USA

[2]Department of Biomedical Engineering, Cleveland Clinic, Cleveland, OH, USA

Abstract

The objective of this work is to examine the development of porcine cartilage by analyzing its mechanical properties, biochemical content, and proteomics at different developmental stages. Cartilage from the knees of fetal, neonatal, juvenile, and mature pigs was analyzed using histology, mechanical testing, biochemical assays, fluorophore-assisted carbohydrate electrophoresis, and bottom-up proteomics. Mature cartilage has 2.2-times the collagen per dry weight of fetal cartilage, and fetal cartilage has 2.1-times and 17.9-times the glycosaminoglycan and DNA per dry weight of mature cartilage, respectively. Tensile and compressive properties peak in the juvenile stage, with a tensile modulus 4.7-times that of neonatal. Proteomics analysis reveals increases in collagen types II and III, while collagen types IX, XI, and XIV, and aggrecan decrease with age. For example, collagen types IX and XI decrease 9.4-times and 5.1-times respectively from fetal to mature. Mechanical and biochemical measurements have their greatest developmental changes between the neonatal and juvenile stages, where mechanotransduction plays a major role. Bottom-up proteomics serves as a powerful tool for tissue characterization, showing results beyond those of routine biochemical analysis. For example, proteomic analysis shows significant drops in collagen types IX, XI, and XIV throughout development, which shows insight into the permanence of cartilage's matrix. Changes in overall glycosaminoglycan content compared to aggrecan and link protein indicate non-enzymatic degradation of aggrecan structures or hyaluronan in mature cartilage. In addition to tissue characterization, bottom-up proteomics techniques are critical in tissue engineering efforts toward repair or regeneration of cartilage in animal models.

Keywords

Cartilage; Articular cartilage; Cartilage development; Bottom-up proteomics

[†]Corresponding author: athens@uci.edu.
[*]These authors contributed equally

Author Contributions

Study concept and design: Bielajew, Donahue, Hu, Athanasiou
Data acquisition and interpretation: All authors
Manuscript drafting, revising, and approval: All authors

Competing Interests

Kyriacos A. Athanasiou and Jerry C. Hu are scientific consultants at Cartilage Inc.

1. Introduction

Cartilage does not heal, and current clinical treatments for cartilage degeneration are palliative, not reparative. This motivates cartilage tissue engineering, which aims to design neotissues for cartilage repair or replacement. Many researchers have attempted to engineer neocartilages by recapitulating aspects of cartilage development, including the self-assembling process which is reminiscent of mesenchymal condensation [1, 2]. Toward ensuring that developmentally accurate neocartilage is produced, developing native cartilage must be characterized — especially its mechanical properties as a function of its biochemical and proteomic content. Through these characterizations, design criteria for tissue-engineered cartilages may be established such that the neocartilage implants are capable of bearing loads experienced by adults in daily activities. Additionally, tissue engineering strategies that mimic developmental processes will be informed by a characterization of these structure-function relationships over developmental time points from fetal to mature tissue.

The extracellular matrix (ECM) content and mechanics of cartilage change during development and aging [3]. Knee articular cartilage forms as a result of endochondral ossification during embryonic development. During this process, mesenchymal condensation occurs which results in an interzone region at the future joint. Chondrogenesis of mesenchymal progenitor cells in the perichondrium region of the interzone leads to formation of early cartilage tissues which will later develop into mature cartilage [4]. This process continues into postnatal development where cartilage continues to mature. Collagens and glycosaminoglycans (GAGs), two main ECM components of cartilage, change in quantity and type throughout this process [5, 6]. For example, collagen type II, the principal collagen subtype of hyaline cartilage, is known to increase with tissue maturity [2, 5], but it is not known how other minor collagen subtypes develop. Along with these biochemical changes, mechanical properties of cartilage are altered throughout development [7–9]. For example, human cartilage reaches peak stiffness between 30 and 50 years of age [10]. After cartilage is fully developed, further age-related ECM changes occur, including proteolytic degradation and other post-translational modifications [11]. Biochemical changes alter mechanical properties of the cartilage; for example, cartilage shear modulus has a strong negative correlation with age and osteoarthritis grade [12]. These age-related changes can result in cartilage degeneration and pathology, affecting approximately nearly 1 in 4 US adults [13]. A promising solution to these age-related degenerative changes is tissue engineering, which is poised to provide a long-term regenerative solution to cartilage ailments toward improving pain and function and enhancing quality of life for patients.

Toward informing design criteria for neocartilage, characterization studies have investigated the biochemical and mechanical properties of cartilage. For example, healthy human articular cartilage has an aggregate modulus of 0.08–2 MPa and tensile modulus of 5–25 MPa, depending on tissue location and depth [3]. These properties arise from the biochemical makeup of cartilage, mainly being composed of collagen type II and GAGs. Cartilage contains 50–75% collagen by dry weight (DW) and 15–30% GAG by DW, including chondroitin sulfate (CS) [3]. However, the subtypes of collagens and GAGs are rarely quantified, especially in developmental studies. This study investigates the proteomic

development of cartilage ECM using bottom-up proteomics for the first time, as well as isomers of CS (chondroitin-6-sulfate, CS6, and chondroitin-4-sulfate, CS4), via fluorophore-assisted carbohydrate electrophoresis (FACE), in addition to biochemical and mechanical characterization.

Prior to the development of human tissue-engineered therapeutics, preclinical studies must be done in animal models. There are many accepted animal models for cartilage. For example, the sheep and horse are suggested by the U.S. Food and Drug Administration for preclinical studies that aim to repair or replace knee cartilage due to the biochemical and mechanical similarities to human cartilage [14]. In developmental biology, the porcine model has long been used due to its similarity to human development [15]; this is best illustrated by its use in anatomy courses from the high school to graduate levels. The porcine model has recently emerged as a model for knee cartilage studies due to its cartilage biomechanics [16]. Additionally, minipigs have been used for their lower terminal weight, which offers practical and financial advantages for long-term studies, including easier handling and less food intake [17]. Here, the porcine model is investigated due to its well-studied developmental pathway and suitability as a cartilage preclinical animal model.

The objective of this work is to interrogate the development of knee articular cartilage by analyzing the mechanics, biochemical content, and proteomics of knee articular cartilage from different aged pigs. The hypothesis of this work is that age-dependent changes in the mechanical, biochemical, and proteomic properties will be observed. Specifically, as a function of developmental age, increases in the tensile and compressive mechanical properties, increases in collagen, and decreases in GAG and DNA will be observed. Increases and decreases in proteomic biomarkers will also be observed; however, the specific targets are not known *a priori*. Toward this objective, a wide breadth of characterization analyses were performed on the cartilage of pigs ranging from fetal to 2+ years, including compressive and tensile mechanical testing; photometric collagen, GAG, and DNA assays; mass spectrometry for collagen crosslinks; FACE for CS isomers; and bottom-up proteomic approaches for cartilage proteins.

2. Methods

2.1 Sample collection

Fresh-frozen whole fetal and neonatal pigs (*Sus scrofa domesticus*, Yorkshire cross, female and male) were purchased from Nebraska Scientific. According to the provided growth chart, the pigs were determined to be of 80d, 90d, or 100d gestational age, or stillborn (neonatal). Knees from juvenile (5–6 month old) and mature (2–3 year old) pigs (*Sus scrofa domesticus*, Yorkshire cross, female and castrated male), culled for purposes unrelated to this research, were purchased from Corona Cattle, Inc. For fetal and neonatal pigs, unilateral (only the right) knee joints were used, and for juvenile and mature pigs, bilateral knee joints were used. Prior to sample collection, juvenile and mature knees were fresh-frozen *en bloc* and subsequently thawed to ensure consistency with fetal and neonatal groups. Knee joint capsules were then opened, and macroscopic joint health of patellofemoral joints was checked to ensure that they were absent of osteoarthritic changes such as osteophytes and cartilage fibrillation or defects. A total of 44 knees were used, as follows: 7 knees

from fetal 80d, 7 knees from fetal 90d, 7 knees from fetal 100d, 7 knees from neonatal, 8 knees from juvenile, and 8 knees from mature pigs. Osteochondral samples were taken from three locations on the condyles with disposable 3 mm diameter biopsy punches as depicted in Figure 1, and subchondral bone was then trimmed off at the tidemark with a scalpel blade. The center of the condyle was defined as the intersection of midpoints of the height and width of each condyle. Punch 1 from the center of the lateral condyle was cut into a dog-bone shape (approximately 0.5 mm width by 1.0 mm thickness) for tensile testing, and the removed portions were used for crosslinks and bottom-up proteomics analyses. Punch 2 from the center of the medial condyle was used for compression testing and histology, with a 2 mm diameter sample (full-thickness, approximately 1 mm in height) from the center used for stress-relaxation test, and the remaining portion used for histology. Punch 3 was taken adjacent to punch 1 as shown in Figure 1, and this full-thickness sample was used for the biochemical analysis, including the collagen, GAG, DNA, and FACE assays. Mechanical testing samples were stored in phosphate-buffered saline after collection and tested within 24 hours.

2.2 Histology

Hematoxylin and eosin (H&E), picrosirius red (PR), and safranin O (SO) histological stains were performed. A full-thickness slice of cartilage was fixed in 10% neutral buffered formalin, processed, embedded in paraffin, sectioned to 5 μm thickness, mounted on microscopy slides, and stained with H&E, PR, or SO, as previously described [18]. For all stains, all samples were stained simultaneously to ensure consistency. Representative images were taken at 20x magnification on a brightfield microscope. All histology slides were reviewed by a histopathologist to ensure quality of staining.

2.3 Mechanical testing

Tensile and compressive mechanical testing was performed, as previously described [19]. Briefly, dog-bone shaped specimens were glued to paper tabs for uniaxial tensile tests. Tabs were gripped in a uniaxial testing machine with a gauge length of 1.55 mm, and samples were subjected to a pull-to-failure test at 1% strain per second. A custom MATLAB code was used to determine the tensile Young's modulus and ultimate tensile strength (UTS) from the engineering stress-strain curves which were generated from force-displacement curves. For compressive stress-relaxation tests, 2 mm diameter tissue punches were subjected to 15 preloading cycles of 5% strain followed by application of 10% and 20% strain held for 600 and 900 seconds, respectively, until relaxation equilibrium. The loading rate was 10% strain per second. The force-displacement curves were fit to a standard linear solid model using a custom MATLAB code to obtain instantaneous modulus and relaxation modulus at both strain levels.

2.4 Photometric biochemical assays for total collagen, GAG, and DNA content

Hydration was measured by comparing the wet weight (WW) to the post-lyophilization DW. Cartilage was digested overnight with papain, and photometric biochemical assays were performed, as previously described [20]. Briefly, overall collagen content (COL) was measured with a modified hydroxyproline assay [21]. GAG content was measured with a

dimethylmethylene blue assay kit, and DNA was measured with a PicoGreen assay kit. The resulting COL, GAG, and DNA values were normalized to both WW and DW.

2.5 Fluorophore assisted carbohydrate electrophoresis (FACE)

Aliquots of the papain digests (50 μL) were lyophilized and subjected to a series of ethanol precipitations and digestion with chondroitinase ABC. The digested disaccharides were fluorescently derivatized with 2-aminoacridone and separated using FACE, as previously described [22]. CS6 and CS4 contents were quantified using ImageJ software measurements of band integrated optical density with CS6 and CS4 standards, and CS6 content was divided by CS4 content to obtain the CS6/CS4 ratio.

2.6 Crosslink quantification and bottom-up proteomics

Collagen crosslink quantification and bottom-up proteomics were performed, as previously described [23]. Briefly, cartilage pieces ~1 mg in WW from the lateral condyle punch were used for both assays. For crosslinks, cartilage pieces were hydrolyzed in HCl, and hydrolysates were subjected to aqueous normal phase chromatography and mass spectrometry with a Waters ACQUITY QDa quadrupole mass spectrometer to quantify pyridinoline (PYR), dihydroxylysinonorleucine (DHLNL), hydroxyproline (OHP), and internal standard pyridoxine. For bottom-up proteomics, cartilage pieces were digested in trypsin then subjected to reverse-phase chromatography and tandem mass spectrometry on a Thermo Fisher Scientific Orbitrap Fusion Lumos mass spectrometer, then label-free quantification was performed with MaxQuant [24] to quantify all identified proteins, normalized to total protein content. Total protein content was determined by dividing the COL/DW from the hydroxyproline assay by the sum of all collagen proteins per total protein, yielding total protein per DW.

2.7 Statistical analysis

Experimental data were analyzed with a one-way analysis of variance (ANOVA) with the factor being tissue age followed by a *post hoc* Tukey's honestly significant difference test. A sample size of 7–8 per group (i.e., one from each knee) was used for mechanical testing, biochemical analysis, and crosslink quantification. For bottom-up proteomics, three randomly selected samples per group were used. Normality was verified by a Shapiro-Wilk test. Statistical analyses were performed in JMP Pro 14, and graphs were generated in GraphPad Prism 9. In all bar graphs, bars represent the mean ± standard deviation, and statistical significance is represented with a connecting letters report; bars that do not share a letter are significantly different from each other. Reported p-values presented in the text refer to multiple pairwise comparisons, all of which are described by the stated p-value inequality. For example, $p<0.0001$ means that all pairwise comparisons yielded p-values below 0.0001.

3. Results

3.1 Histology

Representative histological images from each cartilage age are shown in Figure 2. H&E staining shows the relative hypercellularity of fetal and neonatal cartilage compared to juvenile and mature, which is consistent with DNA content. Throughout cartilage

development, the number of cells decreased and spacing among cells increased. PR staining showed a more intense red staining on the juvenile and mature cartilage than the other groups, which is consistent with the quantitative hydroxyproline assay. All cartilages stained intensely for GAGs with SO.

3.2 Mechanical testing

The mechanical testing results are depicted in Figure 3. For compressive properties, the juvenile cartilage had the highest instantaneous and relaxation moduli ($p<0.01$). For the 10% instantaneous modulus, the juvenile cartilage was 1.5-times that of neonatal cartilage and 3.0-times that of mature cartilage. The other compressive measurements had similar results, with the juvenile cartilage having between 1.4- and 6.9-times the moduli of all other groups. In tensile testing, the juvenile cartilage had the highest tensile Young's modulus of 37.2±20.1 MPa, significantly higher than any of the other groups ($p<0.0001$). This stiffness was 10.5-times that of the fetal 80d cartilage, 4.7-times that of neonatal cartilage, and 3.1-times that of mature cartilage. The juvenile cartilage also had the highest UTS at 15.6±7.1 MPa ($p<0.0001$), over double that of any other cartilage. The fetal tissues had the lowest UTS, which had means ranging from 0.6–1.0 MPa.

3.3 Biochemical content

The biochemical analysis results are shown in Figure 4. COL/DW and COL/WW were significantly greater in the juvenile and mature tissues than in fetal or neonatal tissues ($p<0.0001$). Juvenile and mature cartilages contained about 2.2-times the COL/DW of fetal and neonatal cartilages. While there were no significant differences in GAG/WW among the different age groups, GAG/DW was significantly lower in the juvenile and mature tissues than in the fetal or neonatal tissues ($p<0.01$), dropping about 1.6-times from neonatal to juvenile. DNA/WW and DNA/DW were significantly lower in juvenile and mature tissues than in fetal or neonatal tissues ($p<0.01$). The fetal 80d cartilage had 12.0-times the DNA/DW of juvenile cartilage, and 17.9-times the DNA/DW of the mature cartilage. The hydration of the juvenile and mature tissues was significantly less than that of the younger tissues ($p<0.01$), dropping from a maximum of 87.0±0.7% in the fetal 90d cartilage to a minimum of 75.2±3.8% in the mature cartilage. The CS6/CS4 ratio was significantly higher in the mature cartilage than the other ages ($p<0.001$), at 1.85±1.29, while the other tissues ranged from 0.10±0.03 (fetal 90d) to 0.37±0.10 (juvenile).

3.4 Crosslinks analysis

The crosslink quantification results are shown in Figure 5. There were no significant differences among any tissue ages for PYR/DW or DHLNL/DW. The fetal 80d group had significantly more PYR/OHP than other groups ($p<0.01$) at 12.0±2.1 mmol/mol, but there were no other significant differences among groups, and there were no differences in DHLNL/OHP. The fetal 80d cartilage contained 1.9-times the PYR/OHP of juvenile cartilage, and 1.6-times that of mature cartilage. The maturity ratio, which compares the molar amounts of PYR and DHLNL, did not have any significant differences among tissue ages. The highest mean PYR/DHLNL was in the fetal 80d cartilage (1.4±0.4 mol/mol), while the lowest mean PYR/DHLNL was in the mature cartilage (1.0±0.2 mol/mol), but this difference was not significant.

3.5 Bottom-up proteomics

Over 400 individual proteins were quantified through the bottom-up proteomics approach, which were narrowed down to 42 proteins, including 13 collagen types, that had an intensity of >0.1% per protein in at least one sample. Of the 42 proteins, 15 selected analytes of interest are shown in Figure 6 (the larger list of 42 proteins is presented in Supplementary Table 1). Significant differences were found in several proteomic targets. Collagen types II and III increased with age; aggrecan, collagen types IX, XI, XIV, histone H4, link protein, tenascin, tubulin, and vimentin decreased with age; and collagen types I, VI, and XII did not significantly change with age.

4. Discussion

In this study, the objective was to elucidate the mechanical, biochemical, and proteomic changes in cartilage throughout development by analyzing knee cartilage from fetal, neonatal, juvenile, and mature pigs. The hypotheses that there will be age-dependent increases in collagen and mechanical properties, as well as age-dependent decreases in GAG and DNA were confirmed. The proteomics analysis revealed that as cartilage ages, its collagen profile shows increases in types II and III and decreases in types IX, XI, and XIV. Aggrecan core protein and link protein, both associated with the GAG bottlebrush structure [25], decrease with age. Some intracellular proteins, such as histones, decrease with age, which is expected given the measured decrease in DNA with age. Some collagen types, such as types I, VI, and XII did not change throughout development. As described below, the proteomics analysis yielded insights into cartilage development because of the quantification of individual collagen subtypes, GAG structural components, and cellular proteins, beyond what can be accomplished in traditional assays for collagen, GAG, and DNA.

Throughout cartilage development, mechanical properties increased from fetal to juvenile, then decreased between juvenile and mature time points. The greatest changes occurred between neonatal and juvenile cartilage in most mechanical and biochemical measurements. Specifically, when comparing neonatal to juvenile tissues, the tensile Young's modulus increased 4.7-times, the 20% relaxation modulus increased 2.7-times, the COL/DW increased 2.2-times, and the DNA/DW decreased 8.2-times. With this developmental stage occurring in the few months following birth, it is likely that mechanotransduction and hormones are major drivers of cartilage developmental changes. Once neonates begin to walk, cartilage loading and strain increase, which can lead to ECM synthesis through osmo-mechanosensitive ion channels [26]. Growth hormone, which stimulates growth of articular chondrocytes and contributes to cartilage growth and maturity [27], circulates at high levels in neonatal pigs [28]. Maximum mechanical properties occurred at the juvenile stage; from juvenile to mature cartilage, tensile Young's modulus decreased by 3.1-times, and 20% relaxation modulus decreased 1.8-times. However, these changes were not reflected in biochemical properties; collagen, GAG, and DNA had no significant differences between juvenile and mature cartilages. One potential explanation for the decreases in mechanical properties is that farm pigs have been characterized as a model of spontaneously occurring osteoarthritis, where 80-week old pigs exhibit more lameness and higher chondropathy scores than juvenile pigs, and these degenerative changes worsen as the pigs age to 3–4

years [29]. The mature pigs used in the present study were 2–3 years old, and even though the joints were undamaged to the naked eye, the mechanical properties may be signs of a pre-osteoarthritic state. Rapid weight gain, which is caused by selective breeding and intensive feeding [30], may have led to excessive force and wear on the articular cartilage of the mature pigs, leading to degenerative states that were not detectable via gross observation. Future studies should closely consider not only the biomechanics of weight bearing regions of porcine stifle joint cartilage due to differences compared to humans [31, 32] but also the phenotype of chondrocytes within the matrix through RNA sequencing to gain further insight into this pre-osteoarthritic state.

The existence of different CS isomeric forms and the prevalence and ratios of these isomers in different tissue ECMs suggests tissue specific functionality [33]. Of particular interest is the CS6/CS4 ratio in maturing cartilage. Changes in this ratio may be due to ECM remodeling through cartilage development, or may be an indicator of disease and aging. In previous studies, mature porcine cartilage was shown to contain a very small ratio of CS6/CS4, and a decrease in this ratio is correlated with tissue maturation [2, 34]. However, FACE analysis for this study showed lower CS6/CS4 ratios in less developed tissues and a significant increase in mature samples. This inconsistency with previous experiments may be a result of the previously discussed pre-osteoarthritic state of the mature cartilage, because, as osteoarthritic cartilage degrades, GAGs are cleaved from cartilage ECM and released into synovial fluid [35], which may lead to different sulfation ratios with GAG turnover. With the pre-osteoarthritic state of the mature cartilage in this work, it is likely that many of these GAGs are cleaved from the surface of the cartilage, because the surface zone stains less with SO with increasing age (Figure 2). Further investigation into CS6/CS4 ratios, especially at different cartilage depths, in developmental and disease states is needed to fully understand the spike in the CS6/CS4 ratio for the mature cartilage in this study.

Bottom-up proteomic techniques have recently received attention as critical tools in tissue characterization, capable of simultaneous quantification of hundreds of proteins [36], and been used to show signaling pathways of osteoarthritic diseases [37], to compare different cartilages [23, 38], and to compare the proteome of neocartilage engineered from different aged chondrocytes [39]. While developmental proteomic studies have been performed in mice [40], this study was novel in that it used bottom-up proteomics to show developmental changes in a clinically relevant large animal model for the first time. The hydroxyproline assay showed an increase in overall collagen throughout development, and the proteomics analysis showed that the collagen types that increase are mostly collagen types II and III, which increased by factors of 1.3 and 4.8, respectively, from fetal to mature. Other types of collagen such as types IX and XI, and XIV decreased throughout tissue maturity; types IX and XI dropped by factors of 9.4 and 5.1, respectively, and type XIV dropped from 0.95% in fetal cartilage to <0.01% in mature cartilage (Supplementary Table 1). Collagen types IX and XI are known to decrease with age as finer fibrils mature to thicker and more variably sized fibrils in mature cartilage [41], but the same was not known of collagen type XIV. Collagen type XIV is involved in fibrillogenesis by regulating collagen fibril diameter [42]. Using values reported in Supplementary Table 1 and Figure 6, the sums of the means reported for collagen types IX, XI, and XIV were 17.3% for fetal, 13.8% for neonatal, 3.6% for juvenile, and 2.6% for mature cartilage; the higher proportion of these collagen subtypes

in younger tissue indicates that they are critical for collagen development in cartilage, where fibrils assemble into mature fibers of mainly collagen type II. Radiocarbon dating shows that the collagen matrix of articular cartilage has little to no turnover, and once the collagen type II matrix matures, it is essentially a permanent structure [43]. The drop in collagen types IX, XI, and XIV shown here may either be a cause or an effect of this permanence; either the cartilage loses the tools to rebuild its collagen structure during tissue maturation, or these tools are degraded and replaced as they become no longer needed. The application of bottom-up proteomics techniques to elucidate developmental changes in the collagen profile of cartilage is a novel, exciting aspect of this study that can also be applied to the full cartilage proteome.

The bottom-up proteomics data offer additional insights in non-collagen proteins as well. For example, the amount of aggrecan core protein per total protein dropped 2.6-times from fetal to mature cartilage. This was similar to the 2.1-times drop in GAG/DW across the same ages. This may indicate that entire proteoglycan structures consisting of aggrecan and GAGs are removed from the ECM with aging. Age-related enzymatic degradation of GAG structures typically involve depletion of CS and cleavage of aggrecan without removal of link protein [44]. It is likely that the changes seen here are a result of mostly non-enzymatic breakdown of aggrecan structures or hyaluronan, as these pathways remove link protein [44], and link protein dropped by 5.0-times from fetal to mature, more than the drop in aggrecan. Interestingly, vimentin, an intermediate filament protein, dropped 9.3-times from fetal to mature cartilage, less than the decreases in cellularity seen in the 17.9-times drop in DNA/DW and 54.2-times drop in Histone H4. Thus, the cells that remain in maturing cartilage tissue deposit increasing amounts of vimentin with age. Vimentin intermediate filaments have previously been shown to increase in chondrocytes that experience more mechanical stress [45]; thus, the increase in vimentin per cell shown here (Vimentin/DNA increased 5.2-times from fetal to mature) is likely a result of increases in loading as the animals gain weight and their knees experience greater forces. As cartilage matures, protein markers such as collagen types II and III increased, mirroring the increases in mechanical properties throughout development; however, despite the significant drop-off in mechanics from juvenile to mature cartilage described above, no significant differences were found between these two ages in any proteomic targets except for an increase in collagen type III. It is clear that this pre-osteoarthritic state cannot be sufficiently described by individual biochemical or proteomic biomarkers, and additional studies on cartilage proteomics will be crucial in studying age-related changes that both strengthen cartilage throughout development and weaken it with aging. Proteomic characterization of structural and cellular components of cartilage and other tissues can provide a deeper understanding of tissue development beyond what is offered by routine benchtop assays for collagen, GAG, and DNA, which is of particular use to researchers in the fields of tissue characterization and tissue engineering.

Porcine animal models have recently shown promise as large animal models for cartilage tissue engineering due to similarities in cartilage thickness, and, in the case of the Yucatan minipig, low mature animal weight and mild temperament [19, 46, 47]. While the pigs in this study are not Yucatan minipigs, as used more commonly in orthotopic cartilage large animal studies, the developmental states between the Yorkshire cross breed and the Yucatan

minipig breed would likely be conserved between fetal and juvenile states. Because minipigs gain weight less rapidly and typically are on a more controlled diet within closed research herds, the age-related spontaneous pre-osteoarthritic state may not translate. However, tissue engineers may use the results of this work as benchmarks for preclinical porcine studies. Because of cartilage's role as a mechanical tissue, ideal neocartilages will match the mechanical properties of native cartilage, and the results of this study offer comparison points for tensile and compressive properties. Furthermore, through the elucidation of temporal changes in mechanics, biochemistry, and proteomics, tissue engineers can attempt to more closely mimic the developmental processes of cartilage using tissue engineering techniques toward further improving the mechanical properties of neocartilage. For example, in addition to collagen type II, tissue engineers may also seek to build robust cartilage ECM through collagen types IX, XI, and XIV, which are needed for forming mature collagen type II-based fibers. Modulation, expression, or deposition of these collagen types can conceivably be manipulated to build new cartilage ECM in people who have cartilage degeneration due to injury or disease. Before this is possible, proteomic characterization of human cartilage at different developmental and aging time points is crucial. This work indicates that bottom-up proteomics will continue to be a powerful tool in the fields of tissue characterization, tissue degeneration, and tissue engineering in cartilage and a multitude of other tissues in the body.

Supplementary Material

Refer to Web version on PubMed Central for supplementary material.

Acknowledgments

The authors would like to acknowledge Clinton Yu and Lan Huang at the UCI High-end Mass Spectrometry Facility for assistance with running the bottom-up proteomics analysis.

Funding

This work was funded by NIH grant nos. R01DE015038, R01AR071457, and R01AR067821.

References

[1]. Hu JC, Athanasiou KA, A Self-Assembling Process in Articular Cartilage Tissue Engineering, Tissue Engineering 12(4) (2006) 969–979. [PubMed: 16674308]

[2]. Ofek G, Revell CM, Hu JC, Allison DD, Grande-Allen KJ, Athanasiou KA, Matrix development in self-assembly of articular cartilage, PLoS One 3(7) (2008) e2795. [PubMed: 18665220]

[3]. Athanasiou KA, Darling EM, Hu JC, DuRaine GD, Hari Reddi A, Articular Cartilage, (2017).

[4]. Pacifici M, Koyama E, Iwamoto M, Gentili C, Development of articular cartilage: what do we know about it and how may it occur?, Connect. Tissue Res 41(3) (2000) 175–184. [PubMed: 11264867]

[5]. Morrison EH, Ferguson MW, Bayliss MT, Archer CW, The development of articular cartilage: I. The spatial and temporal patterns of collagen types, J. Anat 189 (Pt 1) (1996) 9–22. [PubMed: 8771392]

[6]. Archer CW, Morrison EH, Bayliss MT, Ferguson MW, The development of articular cartilage: II. The spatial and temporal patterns of glycosaminoglycans and small leucine-rich proteoglycans, J. Anat 189 (Pt 1) (1996) 23–35. [PubMed: 8771393]

[7]. Kempson GE, Relationship between the tensile properties of articular cartilage from the human knee and age, Annals of the Rheumatic Diseases 41(5) (1982) 508–511. [PubMed: 7125720]

[8]. Williamson AK, Chen AC, Sah RL, Compressive properties and function-composition relationships of developing bovine articular cartilage, J. Orthop. Res 19(6) (2001) 1113–1121. [PubMed: 11781013]

[9]. Williamson AK, Chen AC, Masuda K, Thonar EJMA, Sah RL, Tensile mechanical properties of bovine articular cartilage: variations with growth and relationships to collagen network components, J. Orthop. Res 21(5) (2003) 872–880. [PubMed: 12919876]

[10]. Ding M, Dalstra M, Linde F, Hvid I, Mechanical properties of the normal human tibial cartilage-bone complex in relation to age, Clin. Biomech 13(4–5) (1998) 351–358.

[11]. Lotz M, Loeser RF, Effects of aging on articular cartilage homeostasis, Bone 51(2) (2012) 241–248. [PubMed: 22487298]

[12]. Peters AE, Akhtar R, Comerford EJ, Bates KT, The effect of ageing and osteoarthritis on the mechanical properties of cartilage and bone in the human knee joint, Sci. Rep 8(1) (2018) 5931. [PubMed: 29651151]

[13]. Barbour KE, Helmick CG, Boring M, Brady TJ, Vital Signs: Prevalence of Doctor-Diagnosed Arthritis and Arthritis-Attributable Activity Limitation - United States, 2013–2015, MMWR Morb Mortal Wkly Rep 66(9) (2017) 246–253. [PubMed: 28278145]

[14]. E. Center for Biologics, Research, IDEs & INDs for Products to Repair or Place Knee Cartilage, (2019).

[15]. Book SA, Bustad LK, The Fetal and Neonatal Pig in Biomedical Research, Journal of Animal Science 38(5) (1974) 997–1002. [PubMed: 4596894]

[16]. Cone SG, Warren PB, Fisher MB, Rise of the Pigs: Utilization of the Porcine Model to Study Musculoskeletal Biomechanics and Tissue Engineering During Skeletal Growth, Tissue Eng. Part C Methods 23(11) (2017) 763–780. [PubMed: 28726574]

[17]. Vapniarsky N, Aryaei A, Arzi B, Hatcher DC, Hu JC, Athanasiou KA, The Yucatan Minipig Temporomandibular Joint Disc Structure–Function Relationships Support Its Suitability for Human Comparative Studies, Tissue Engineering Part C: Methods 23(11) (2017) 700–709. [PubMed: 28548559]

[18]. Kwon H, O'Leary SA, Hu JC, Athanasiou KA, Translating the application of transforming growth factor-β1, chondroitinase-ABC, and lysyl oxidase-like 2 for mechanically robust tissue-engineered human neocartilage, J. Tissue Eng. Regen. Med 13(2) (2019) 283–294. [PubMed: 30557915]

[19]. Vapniarsky N, Aryaei A, Arzi B, Hatcher DC, Hu JC, Athanasiou KA, The Yucatan Minipig Temporomandibular Joint Disc Structure-Function Relationships Support Its Suitability for Human Comparative Studies, Tissue Eng. Part C Methods 23(11) (2017).

[20]. Gonzalez-Leon EA, Bielajew BJ, Hu JC, Athanasiou KA, Engineering self-assembled neomenisci through combination of matrix augmentation and directional remodeling, Acta Biomater 109 (2020) 73–81. [PubMed: 32344175]

[21]. Cissell DD, Link JM, Hu JC, Athanasiou KA, A Modified Hydroxyproline Assay Based on Hydrochloric Acid in Ehrlich's Solution Accurately Measures Tissue Collagen Content, Tissue Eng. Part C Methods 23(4) (2017) 243–250. [PubMed: 28406755]

[22]. Calabro A, Midura R, Wang A, West L, Plaas A, Hascall VC, Fluorophore-assisted carbohydrate electrophoresis (FACE) of glycosaminoglycans, Osteoarthritis Cartilage 9 Suppl A (2001) S16–22. [PubMed: 11680680]

[23]. Bielajew BJ, Hu JC, Athanasiou KA, Methodology to Quantify Collagen Subtypes and Crosslinks: Application in Minipig Cartilages, Cartilage (2021) 19476035211060508.

[24]. Cox J, Mann M, MaxQuant enables high peptide identification rates, individualized p.p.b.-range mass accuracies and proteome-wide protein quantification, Nature Biotechnology 26(12) (2008) 1367–1372.

[25]. Pomin VH, Mulloy B, Glycosaminoglycans and Proteoglycans, Pharmaceuticals 11(1) (2018).

[26]. Sanchez-Adams J, Leddy HA, McNulty AL, O'Conor CJ, Guilak F, The mechanobiology of articular cartilage: bearing the burden of osteoarthritis, Curr. Rheumatol. Rep 16(10) (2014) 451. [PubMed: 25182679]

[27]. Tsukazaki T, Matsumoto T, Enomoto H, Usa T, Ohtsuru A, Namba H, Iwasaki K, Yamashita S, Growth hormone directly and indirectly stimulates articular chondrocyte cell growth, Osteoarthritis Cartilage 2(4) (1994) 259–267. [PubMed: 11550711]

[28]. Althen TG, Gerrits RJ, Pituitary and serum growth hormone levels in Duroc and Yorkshire swine genetically selected for high and low backfat, J. Anim. Sci 42(6) (1976) 1490–1497. [PubMed: 931824]

[29]. Macfadyen MA, Daniel Z, Kelly S, Parr T, Brameld JM, Murton AJ, Jones SW, The commercial pig as a model of spontaneously-occurring osteoarthritis, BMC Musculoskelet. Disord 20(1) (2019) 70.

[30]. Reiland S, The effect of decreased growth rate on frequency and severity of osteochondrosis in pigs, Acta Radiol. Suppl 358 (1978) 107–122. [PubMed: 233591]

[31]. Proffen BL, McElfresh M, Fleming BC, Murray MM, A comparative anatomical study of the human knee and six animal species, Knee 19(4) (2012) 493–9. [PubMed: 21852139]

[32]. Takroni T, Laouar L, Adesida A, Elliott JA, Jomha NM, Anatomical study: comparing the human, sheep and pig knee meniscus, J Exp Orthop 3(1) (2016) 35. [PubMed: 27928740]

[33]. López-Álvarez M, López-Senra E, Valcárcel J, Vázquez JA, Serra J, González P, Quantitative evaluation of sulfation position prevalence in chondroitin sulphate by Raman spectroscopy, Journal of Raman Spectroscopy 50(5) (2019) 656–664.

[34]. Volpi N, Disaccharide mapping of chondroitin sulfate of different origins by high-performance capillary electrophoresis and high-performance liquid chromatography, Carbohydrate Polymers 55(3) (2004) 273–281.

[35]. Kulkarni P, Deshpande S, Koppikar S, Patil S, Ingale D, Harsulkar A, Glycosaminoglycan measured from synovial fluid serves as a useful indicator for progression of Osteoarthritis and complements Kellgren–Lawrence Score, BBA Clinical 6 (2016) 1–4. [PubMed: 27331021]

[36]. Bielajew BJ, Hu JC, Athanasiou KA, Collagen: quantification, biomechanics, and role of minor subtypes in cartilage, Nat Rev Mater 5(10) (2020) 730–747. [PubMed: 33996147]

[37]. Lei J, Amhare AF, Wang L, Lv Y, Deng H, Gao H, Guo X, Han J, Lammi MJ, Proteomic analysis of knee cartilage reveals potential signaling pathways in pathological mechanism of Kashin-Beck disease compared with osteoarthritis, Sci. Rep 10(1) (2020) 6824. [PubMed: 32322000]

[38]. Önnerfjord P, Khabut A, Reinholt FP, Svensson O, Heinegård D, Quantitative proteomic analysis of eight cartilaginous tissues reveals characteristic differences as well as similarities between subgroups, J. Biol. Chem 287(23) (2012) 18913–18924. [PubMed: 22493511]

[39]. Donahue RP, Nordberg RC, Bielajew BJ, Hu JC, Athanasiou KA, The effect of neonatal, juvenile, and adult donors on rejuvenated neocartilage functional properties, Tissue Eng Part A (2021).

[40]. Wilson R, Norris EL, Brachvogel B, Angelucci C, Zivkovic S, Gordon L, Bernardo BC, Stermann J, Sekiguchi K, Gorman JJ, Bateman JF, Changes in the chondrocyte and extracellular matrix proteome during post-natal mouse cartilage development, Mol Cell Proteomics 11(1) (2012) M111 014159.

[41]. Eyre D, Collagen of articular cartilage, Arthritis Res 4(1) (2002) 30–35. [PubMed: 11879535]

[42]. Ansorge HL, Meng X, Zhang G, Veit G, Sun M, Klement JF, Beason DP, Soslowsky LJ, Koch M, Birk DE, Type XIV Collagen Regulates Fibrillogenesis: PREMATURE COLLAGEN FIBRIL GROWTH AND TISSUE DYSFUNCTION IN NULL MICE, J. Biol. Chem 284(13) (2009) 8427–8438. [PubMed: 19136672]

[43]. Heinemeier KM, Schjerling P, Heinemeier J, Møller MB, Krogsgaard MR, Grum-Schwensen T, Petersen MM, Kjaer M, Radiocarbon dating reveals minimal collagen turnover in both healthy and osteoarthritic human cartilage, Sci. Transl. Med 8(346) (2016) 346ra90.

[44]. Roughley PJ, Mort JS, The role of aggrecan in normal and osteoarthritic cartilage, J Exp Orthop 1(1) (2014) 8.

[45]. Hernandez PA, Wells J, Usheva E, Nakonezny PA, Barati Z, Gonzalez R, Kassem L, Henson FMD, Early-Onset Osteoarthritis originates at the chondrocyte level in Hip Dysplasia, Scientific Reports 10(1) (2020).

[46]. Goetz JE, Fredericks D, Petersen E, Rudert MJ, Baer T, Swanson E, Roberts N, Martin J, Tochigi Y, A clinically realistic large animal model of intra-articular fracture that progresses

to post-traumatic osteoarthritis, Osteoarthritis Cartilage 23(10) (2015) 1797–1805. [PubMed: 26033166]

[47]. Frisbie DD, Cross MW, McIlwraith CW, A comparative study of articular cartilage thickness in the stifle of animal species used in human pre-clinical studies compared to articular cartilage thickness in the human knee, Vet. Comp. Orthop. Traumatol 19(3) (2006) 142–146. [PubMed: 16971996]

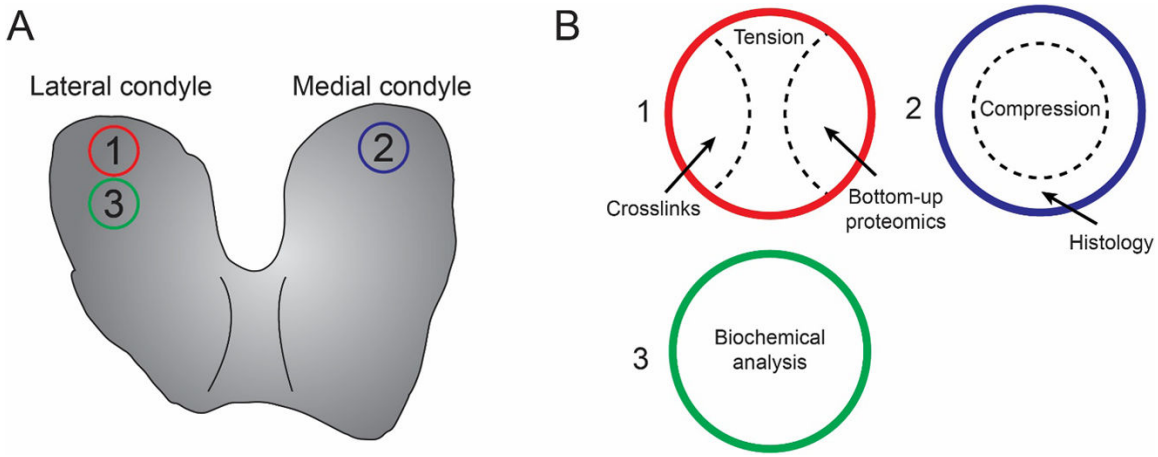

Figure 1.

Sample collection diagram. This illustration shows the (A) lateral and medial condyles with punch locations (not to scale) and (B) sample locations within each punch.

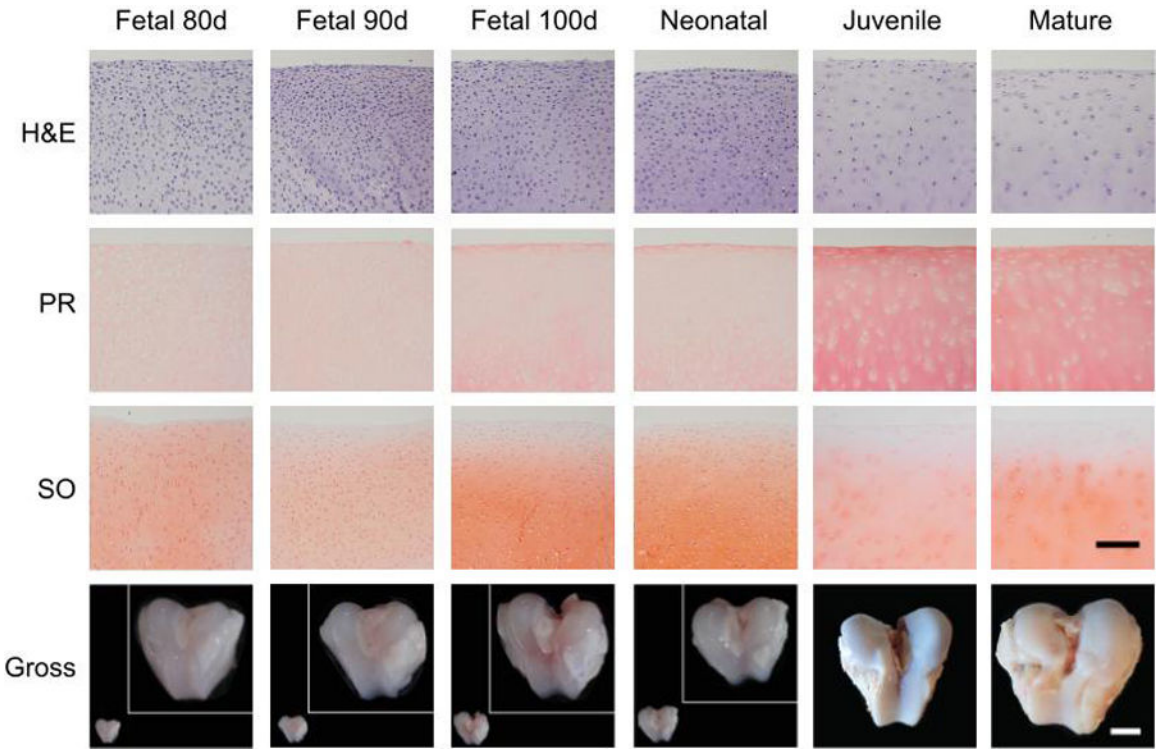

Figure 2.

Representative histology and gross morphology images for porcine articular cartilage of different developmental ages. Fetal and neonatal gross morphology images are shown in actual size (bottom left) and zoomed in (inset). Juvenile and mature are shown in actual size. Scale bars: histology, 100 μm, gross morphology, 2 cm. H&E, hematoxylin and eosin. PR, picrosirius red. SO, safranin O.

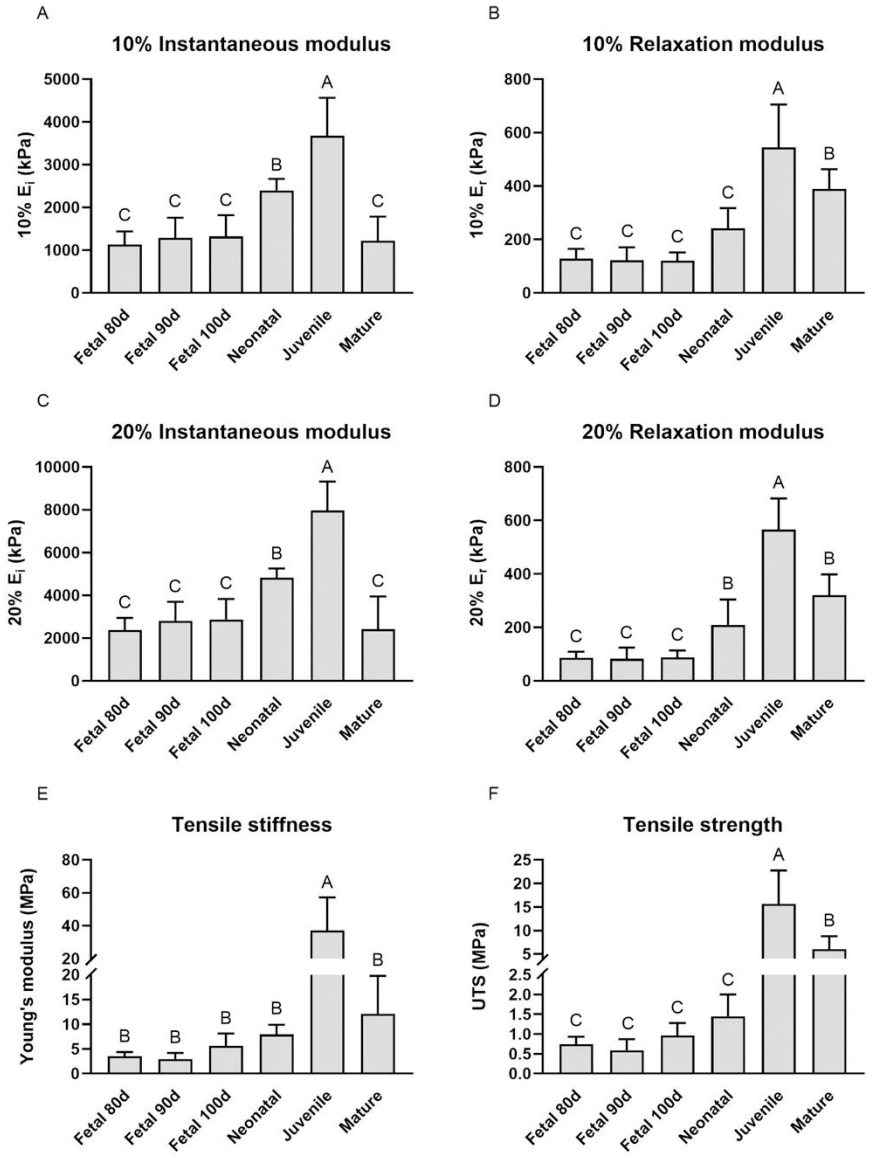

Figure 3.

Mechanical results for porcine articular cartilage of different developmental ages. These graphs show the (A) 10% instantaneous modulus, (B) 10% relaxation modulus, (C) 20% instantaneous modulus, (D) 20% relaxation modulus, (E) tensile stiffness, and (F) tensile strength. Ei, instantaneous modulus. Er, relaxation modulus. UTS, ultimate tensile strength. Bars that do not share a letter are significantly different from each other.

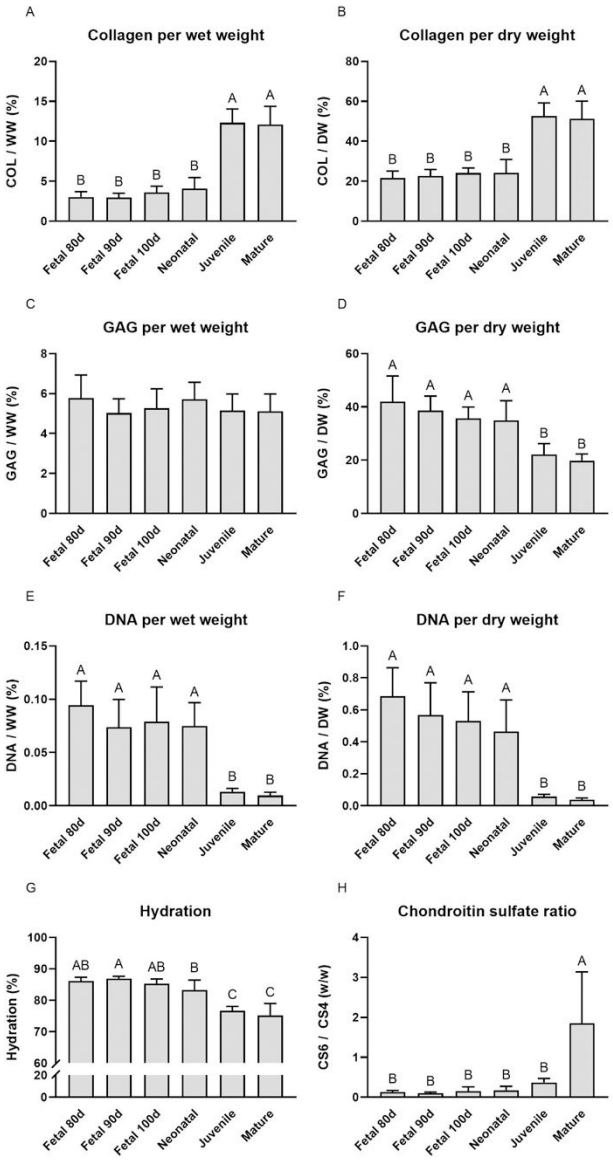

Figure 4.

Biochemical results for porcine articular cartilage of different developmental ages. (A, B) Collagen per wet weight and dry weight, respectively. (C, D) Glycosaminoglycan per wet weight and dry weight, respectively. (E, F) Double-stranded DNA per wet weight and dry weight, respectively. (G) Hydration of tissue. (H) Ratio of chondroitin 6-sulfate to chondroitin 4-sulfate. COL, collagen. WW, wet weight. DW, dry weight. GAG, glycosaminoglycan. CS6, chondroitin-6-sulfate. CS4, chondroitin-4-sulfate. Bars that do not share a letter are significantly different from each other.

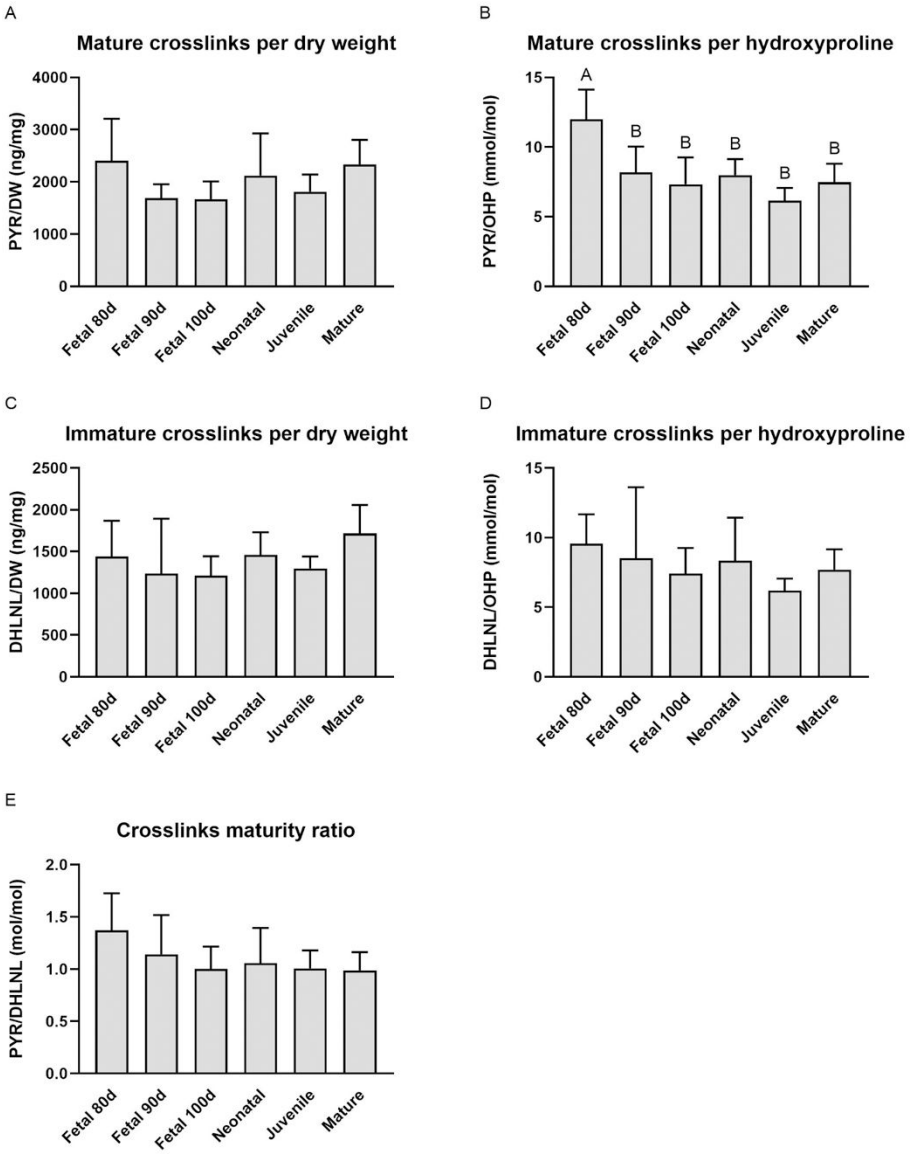

Figure 5.

Crosslink quantification results for porcine articular cartilage of different developmental ages. (A, B) Mature pyridinoline crosslinks normalized to dry weight and hydroxyproline, respectively. (C, D) Immature dihydroxylysinonorleucine crosslinks normalized to dry weight and hydroxyproline, respectively. (E) Crosslinks maturity ratio, calculated as the molar ratio of pyridinoline to dihydroxylysinonorleucine. PYR, pyridinoline. DW, dry weight. OHP, hydroxyproline. DHLNL, dihydroxylysinonorleucine. Bars that do not share a letter are significantly different from each other.

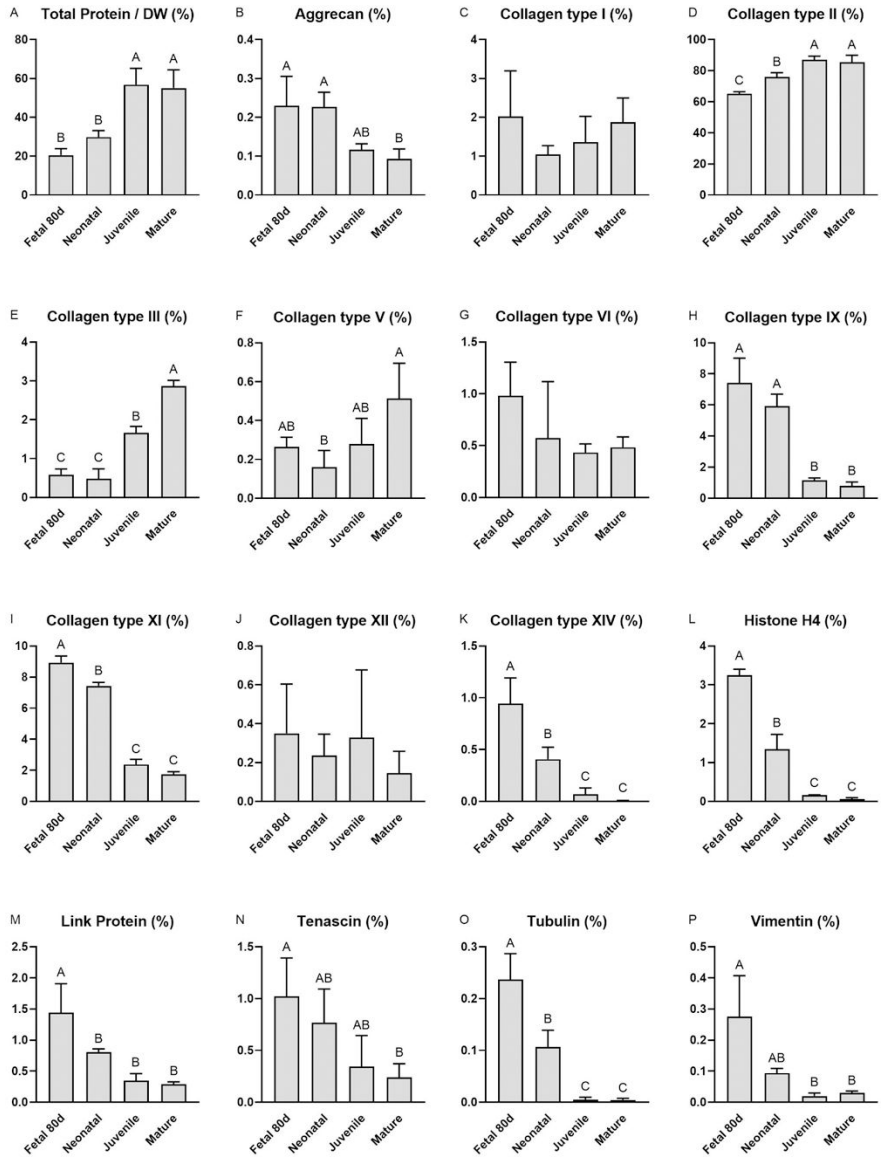

Figure 6.

Bottom-up proteomic results for porcine articular cartilage of different developmental ages. Orbitrap results showing (A) total protein content and (B-P) 15 different proteins of interest in different ages of porcine cartilage. All proteins are normalized to total protein content and calculated as a percentage. A table containing averaged data from the four ages can be found in Supplementary Table 1. DW, dry weight. Bars that do not share a letter are significantly different from each other.